

## Shafiqur Rehman

Interdisciplinary Research Center for  
Renewable Energy and Power Systems  
The Research Institute, King Fahd  
University of Petroleum and Minerals,  
Dhahran-31261,  
Saudi Arabia

## Umar T. Salman

Electrical Engineering Department  
KFUPM, Dhahran-31261,  
Saudi Arabia

## Mohammed A. Mohandes

Electrical Engineering Department  
KFUPM, Dhahran-31261,  
Saudi Arabia

## Fahad A. Al-Sulaiman

Interdisciplinary Research Center for  
Renewable Energy and Power Systems  
The Research Institute, King Fahd  
University of Petroleum and Minerals,  
Dhahran-31261,  
Saudi Arabia

## Sunday Adetona

Department of Electrical and Electrical  
Engineering, University of Lagos, Akok,  
Lagos  
Nigeria

## Luai M. Alhems

Applied Research Center for Metrology,  
Standards, and Testing  
The Research Institute, KFUPM, Dhahran-  
31261, Saudi Arabia

## Mohammed A. Baseer

Department of Mechanical & Manufacturing  
Engineering Technology, Jubail Industrial  
College, Jubail,  
Saudi Arabia

# Wind Speed Prediction Based on Long-Short Term Memory using Nonlinear Autoregressive Neural Networks

*Globally, wind power is a technologically matured and commercially accepted technology. However, intermittent and fluctuating wind speed makes it difficult to connect it directly to the grid. It becomes less attractive from the quality and continuous power supply point of view. Nevertheless, the wind speed is affected by meteorological parameters like temperature, pressure, and relative humidity and may be predicted better using all of these parameters or some of the theses as inputs. Since the weather conditions of a particular month repeat approximately after ten years and sometimes even year to year depending on geographical location. This study investigates the errors associated with predicting the wind speed of a particular calendar month using the historical data of the same calendar month in the previous years. Authors propose a strategy for long-term prediction of wind speed based on two nonlinear autoregressive neural network models, (i) nonlinear autoregressive neural network and (ii) nonlinear autoregressive neural networks with exogenous inputs. The models are developed by training the networks with hourly mean wind speed values for seven years, from 2011 to 2017, for three sites in the Eastern Province of Saudi Arabia. These models are used to predict the wind speed for 2018, and the results are compared with the measured data. Both models' effectiveness is evaluated by considering the impact of the exogenous parameters (temperature and atmospheric pressure). The study found that the prediction accuracy of wind speed in long-term forecasting depends not only on the location but also on the repeatability of training samples across the years.*

**Keywords:** Errors, forecasting, nonlinear autoregressive neural network wind speed, wind power.

## 1. INTRODUCTION

Wind power is proving to be a competitive alternative source of energy to the conventional fossil fuel-based generation and its suitability as a distributive power source for isolated micro-grids [1–4]. A continuous campaign is being emphasized for increased wind power capacity and the existing energy mix to mitigate the greenhouse gas (GHG) emissions responsible for environmental pollution. Evidently, many research articles focusing on multi-gigawatts wind power generation facilities across the globe are being published. It is reported that wind power has emerged as one of the most competitive renewable power generation technologies in recent decades [5–9]. Although, the stability of wind power integration into the grid is still a challenge due to the intermittent nature of the wind speed. Many of such challenges have been addressed by researchers and reported in the literature. It is reported that weather variation of a Calendar month repeats itself in another

year and affects the seasons [10–14]. It is said that climate change is a significant factor responsible for the variation of wind speed [15]. It is further stated that there may be less increase in wind speed in urban areas than in rural areas due to urbanization activities. Jiang et al. [16] reported that urbanization reduces the wind speed in cities because of the increased surface roughness. The study reported that wind speed is decreased by 0.01m/s every ten years [16]. Li et al. [17] studied wind speed trends using the homogenized wind speed dataset obtained from the Greater Beijing Region between 1956 and 2008. They showed that wind speed decreased in all regions, and the highest reduction was recorded near the city center. Nevertheless, wind speed is affected by meteorological parameters such as ambient temperature, pressure, and relative humidity and may be predicted more accurately using these parameters.

Hitherto, there are two ways of tackling the problem of randomness and uncertainty of wind power. One way is to increase the size of the installed capacity above the intended amount originally proposed and ensure an adequate rotating reserve of conventional units to account for the impact of fluctuations of wind power integration to the grid [18]. The second method is

Received: December 2021, Accepted: March 2022

Correspondence to: Dr Shafiqur Rehman  
Interdisciplinary Research Center for Renewable  
Energy and Power Systems (IRC-REPS)  
E-mail: srehan@kfupm.edu.sa

doi:10.5937/fme2201260R

© Faculty of Mechanical Engineering, Belgrade. All rights reserved

FME Transactions (2022) 50, 260-270 260

to forecast the wind speed and hence the wind power accurately ahead of time to help the grid operators plan power dispatch properly, assure continuity of power availability, and enhance contain the power economy [19].

Wind speed forecasting has been divided into short-, medium, and long-term periods. The short-term forecasting of wind speed is considered as advanced prediction between 1-48 hours. Short-term forecasting is important for economic planning of wind power generation. It helps the power utility operators to plan adequately for their operation mode, especially when demand is known. Some important formulations and applications of short-term wind speed forecasting are presented in [18–24]. Medium forecasting of wind speed spans from 48 to 72 hours. In long-term forecasting, the advance time of forecast is any time above 72 hours [25]. Since, the wind speed directly influences the power output, long-term forecasting becomes important for wind power plants development. It helps monitor the scheduling of wind power generation and energy management in wind farms.

The fundamental principle of time series forecasting accuracy largely depends on detecting the sub-patterns in the time series and the historical incidents [14]. Time series patterns possess characteristics such as random variations, cyclic patterns, level shifts, and seasonality. Furthermore, fluctuations existing in the time series data are also periodic. These fluctuations can be detected and eliminated by studying the existence of trends within the series. This can be achieved by the removal of seasonality using seasonality decomposition methods. Seasonal decomposition is usually carried out before the application of forecasting algorithms. The stages involved in seasonality decomposition for time series are reported in [14].

Tyler et al. [26] presented two variants of artificial networks: nonlinear autoregressive neural network and nonlinear autoregressive network with exogenous inputs using hourly data of one year. Using a hybrid data processing strategy, Zhongshan et al. [27] developed models for forecasting wind speed. The study enhanced the forecast model by combining complement ensemble empirical mode decomposition (CEEMD) and a wind-driven optimization technique. The wind speed time series was first decomposed into many intrinsic mode functions using the CEEMD, and each intrinsic mode function was used to forecast using back propagation neural networks. The forecasted intrinsic mode functions were then combined as the final predicted values. The strategy was only applied for a short-term forecasting ahead of 10- and 30-minutes. The results showed that the model improved the forecasting accuracy of wind speed for the short-term prediction. However, extending such a study for long-term wind speed forecast would be interesting.

In [28], the authors proposed Hammerstein model for forecasting wind speed for 1-24 hours horizon. The study used the heterogeneous autoregressive (HAR) model to capture wind speed time series dynamics. The result proved that the HAR model has a high propensity to outperform both multilayer perception (MLP) and autoregressive integrated moving average (ARIMA)

models judged by the error metrics. The HAR model was suitable for the hourly forecast of wind speed without evidence to prove otherwise for long-term wind speed prediction.

Barbounis et al. [25], considered up to 72 hours ahead prediction of wind speed as long-term prediction. The study employed three recurrent networks algorithms to predict wind speed using wind speed and wind direction obtained from the atmospheric modeling system SKIRON for four different stations approximately 30,000 m away from the wind turbine clusters. The algorithms included infinite impulse response multilayer perception (IIR-MLP), diagonal recurrent neural network (DRNN), and local activation feedback recurrent (LAF-MLN) models. The results showed that the suggested strategies under the IIR-MLP and DRNN performed better than static algorithms. Furthermore, the study proposed two new online learning strategies for updating the RNN using the recursive recurrent error algorithm. The learning algorithms ensured improvement in the learning phase and improved the accuracy of the models.

A comparative study of the activation function of nonlinear autoregressive neural networks (NARNN) and nonlinear autoregressive exogenous neural networks (NARXNN) for long-term wind speed prediction was reported in [1]. The study provided 30 days ahead forecast of wind speed using data collected from the different metrological stations in Malaysia. The study compared the performance of two activation functions (logsig and tansig) for NARNN and NARXNN models. It revealed that tansig performed better than logsig in terms of minimum prediction errors and transfer functions for the two neural network (NN) models. Similarly, Barbounis et al. [29] demonstrated the effectiveness of a locally recurrent multilayer network using the recursive prediction error (RPE). The model was better than the atmospheric and time series models. Moreover, a global recursive prediction error (GRPE) was developed and partitioned into four sub-problems to reduce the storage requirement and computational complexity.

Neural network-based algorithms were used to develop data fusion algorithms to predict the wind speed trends in the future year. Azad et al. [30] compared the performance of different neural network approaches with classical methods for long-term hourly forecast of wind speed. Judged by MAE and MSE error metrics, it was concluded that the hybridization of different NN algorithms would potentially improve the learning and forecasting performance for long-term wind speed predictions.

## 2. WIND ENERGY IN SAUDI ARABIA

Seasonal variation in Saudi Arabia, like many countries, is expressed in four climatic seasons, which are Spring (Mid-March to Mid-June), Summer (Mid-June to Mid-September), and Autumn (Mid-September to Mid-December), and Winter (Mid-December to Mid-March)[31]. From winter breeze in January to peak desert heat in August, the country experiences different weather changes across the cities and regions. High

wind speed is usually experienced in the winter and summer months. Surprisingly, some of the Eastern Province cities of Saudi Arabia experience high wind speeds during the Summer months (June, July, and August) due to the summer breeze and sandstorms [6,7]. Figure 1 shows the hourly wind speed variation during January and June of 2017 obtained from the metrological station in Khafji. The figure demonstrates the seasonal variation of wind speed at Khafji. These characteristics are mimicked by other metrological parameters that influence wind speed variation throughout the year. This paper investigates the impact of these variations on the long-term wind speed forecasting.

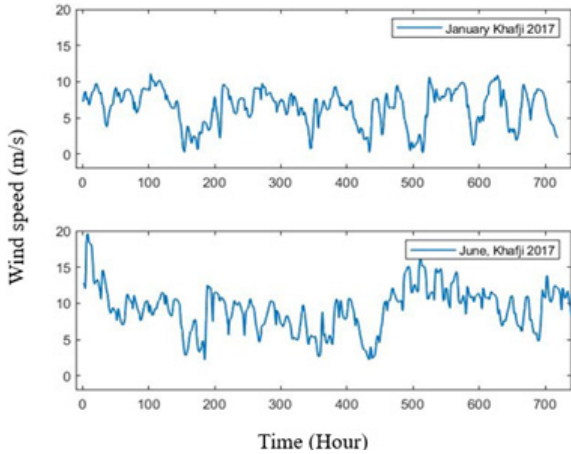


Figure 1. Wind speed measured at 50m height; Khafji, 2017.

## 2.1 Data Preparation

Each meteorological parameter (such as wind speed, ambient temperature, and pressure) is modeled as time series for input to the models. These samples are made of  $n$  observations  $[x_1, x_2, \dots, x_n]$  which are used as input to predict the wind speed ahead of time. The wind speed forecasts will be made a year ahead. This means that the input time series is a function of the past values of 12 calendar months. For each sample, the input training data is modeled as a function  $F(\cdot)$ , given by equation (1):

$$x_{1,t} = F(x_{i,t1}, x_{i,t2}, \dots, x_{i,t-1}) \quad (1)$$

where  $x_{i,t}$  is defined as follows:

$$x_{i,t} = \frac{x_i(t) + x_i(t-1)}{2} \quad (2)$$

where  $i$  is the number of input parameters considered and  $t$  is the total number of sample observations.

## 3. METHODOLOGY

### 3.1 Artificial Neural Network (ANN)

ANN architecture consists of node properties, neurons, connecting strength, and updating rules [32]. Neurons can learn, which can be used to verify the future values [33]. ANNs are used to address complex nonlinear problems in real-life [33]. An ANN model is comprised of components like weights ( $w_{ij}$ ), connecting links, bias ( $b_j$ ), and activation function  $f(\cdot)$  [19]. These input  $x_i$

parameters are related to the output  $y_j$ , as shown in Figure 2. Each input value,  $x_i$  is multiplied by the weight,  $w_{ij}$  and added to the bias  $b_j$  to provide the output  $s_j$ , eq. (3). This output  $s_j$  is applied to the activation function to find the final output  $y_j$ . Examples of activation functions include linear, sigmoid, Gaussian, and Gaussian complements. This function can be selected based on particular problem. The function of the bias is to decrease the effect of the increasing value of  $s_j$ .

$$S_j = \sum_{k=1}^i w_{jk} * x_k + b_j \quad (3)$$

where  $j$  and  $k$  are the numbers neurons and synapses, respectively.

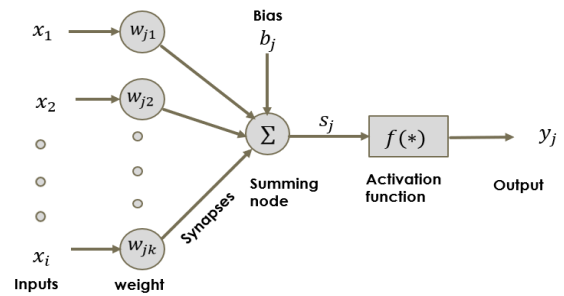


Figure 2. Structure of a neuron.

This study proposes the nonlinear autoregressive neural network (NARNN) and nonlinear autoregressive neural network with exogenous inputs (NARXNN) models. A typical structure of a NARNN is shown in Figure 3. The structure consists of an input  $[y(t-d)]$ , output  $\tilde{y}(t)$ , and hidden layer nodes and the connecting lines. Here  $d$  represents past values of time series used to predict the wind speed ahead of time. The input node is also the feedback node. In developing the NARNN and NARNNX\* models, the predicted time series  $\tilde{y}(t)$  is the wind speed and the external time series included in the input,  $x(t)$  is the exogenous input. The exogenous inputs used in the present work are ambient temperature and pressure.

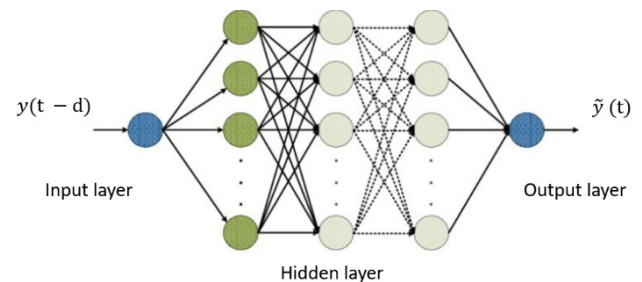


Figure 3. A typical structure of a NARNN.

### 3.2 Nonlinear autoregressive neural network (NARNN)

The NARNN is a multilayer feed-forward NN which includes the input and output layers and one or more hidden layers. The output layer/s is/are usually in-between the input and output layers. The number of neurons in the input layer is the same as training inputs, while the number of neurons in the output layer is equal to the target samples. The optimal number of neurons

can be obtained by a simple trial and error method[32]. For NARNN, the inputs  $x_i$ ,  $[x_1, x_2, x_3]$  is comprised of only wind speed as the training parameter. There are four vectors in each of the three input training observations (i.e.  $n = 12$ ).

For NARXNN\* procedure, each input  $x_i$  has its number of vectors increased by 24 for NARXNN1 by 12 for NARXNN2 as explained in sub-sections 4.1.1, 4.1.2, and 4.1.3. The meteorological parameters considered here are temperatures at 10 m and 2 m and atmospheric pressure near ground level. The reason for considering temperatures at two different levels is that the differences in temperature with height create pressure gradient force, which affects the wind speed [19].

#### 4. PROBLEM FORMULATION

The training data set consists of inputs and targets. The input parameters are the hourly mean wind speed (HWS), ambient temperatures at 10m and 2m and pressure for two months (January and June) of the previous four years, taking two years at a step (Figure 4). The training sample includes the data from 2011 to 2015 and the testing data for years from 2015 to 2017. The training and the testing steps are explained in the following subsections.

##### 4.1 Training Parameters

Three cases are investigated in this study and are explained in the subsequent text. These cases are based on selecting training parameters as described in Figure 5.

**4.1.1 Case 1:** In case of NARNN, the input vector is made of three sets of historical wind speed values from the previous four years measured at 50 m height. These input vectors are  $[x_1, x_2, x_3]$ . Where  $x_1, x_2, x_3$  include all the HWS values for January and June of 2011 and 2012, 2012 and 2013, and 2013 and 2014, respectively. Each vector  $x_1, x_2$ , and  $x_3$  has four input vectors, two from each year for January and June so that the total vectors in the training input becomes 12. The target,  $y_i$ , of the NARNN comprises measured HWS values for January and June 2015.

**4.1.2 Case 2:** This is the first case of NARXNN\* with model NARXNN1. The total inputs include all the values in the NARNN and two more vectors containing temperatures measured at 10 m and 2 m. In this case, the total vectors in each input set become 12, and the new training input set has a total of 36 feature vectors. The target,  $y_i$  of the NARXNN1 consists of measured HWS for January and June 2015 and is same for all the cases.

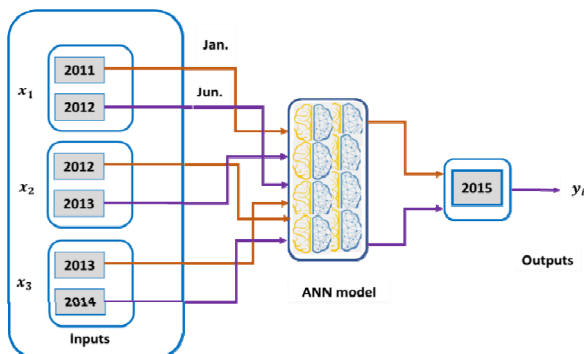


Figure 4. Architecture of the ANN showing the training input and the targets.

**4.1.3 Case 3:** In this case, the model is NARXNN2, the input has all the vectors as in models NARNN, NARXNN1, and additional vectors comprised of atmospheric pressure for January and June. The total input vectors in the training inputs  $[x_1, x_2, x_3]$  become 48. The target sample remains the same measured wind speed values for the year 2015.

##### 4.2 Testing Parameters

The testing input  $sx_t$ , consists of new sets of input vectors. The new input vectors are obtained from the data for the years 2014 to 2017 for January and June. This ensures that the data used for the testing is entirely new and will be used for the final wind speed prediction. The testing input vectors are similar to those of the training data sets described in Section 4.1 for all the cases. For example,  $[xt_1, xt_2, xt_3]$  represent the testing input features comprised of the combination of wind speed such that the vectors in  $xt_1$  are obtained from 2014 & 2015,  $xt_2$  from the 2015 & 2016, and  $xt_3$  from 2016 & 2017 data sets. The architecture of the training and testing samples and predicted values for 2011 to 2018 are depicted in Figure 6. Finally, the test's output results are the forecasted wind speeds for the year 2018, in each case. The output from all the cases is compared with the measured wind speed values for 2018. Furthermore, the results of each case are compared, and the effect of exogenous parameters on the predicted wind speed is studied.

##### 4.3 Forecast Errors

The forecast error is the difference between the measured and the forecasted values. The error metrics are used to evaluate the performance of the proposed models. The performance evaluation metrics used in this study include the mean absolute error (MAE), mean squared error (MSE), and root-mean-squared error (RMSE) and are calculated using the equations (4-6).

$$MAE = \frac{\sum_{t=1}^N |e_t|}{N} \quad (4)$$

$$MSE = \frac{\sum_{t=1}^N e_t^2}{N} \quad (5)$$

$$RMSE = \sqrt{\left\{ \frac{\sum_{t=1}^N e_t^2}{N} \right\}} \quad (6)$$

$I_t$  is the absolute difference between the forecasted and the measured wind speed values for the year 2018, and  $N$  is the number of observations.

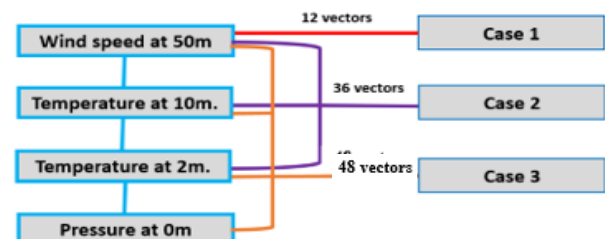


Figure 5. Description of the training parameters and input vectors.

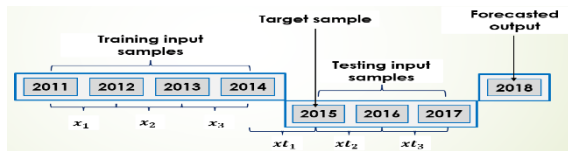


Figure 6. Architecture of the proposed long-term wind forecasting.

#### 4.4 Accuracy of Long-Term Wind Power Forecasting

The accuracy of long-term wind forecasting should not be compared with short-term forecasting because the latter has smaller forecasting errors. It is reported that the error accuracy of long-term wind speed forecasting varies from 25% to 40%[34]. These errors are not only due to a long period of forecast but may also be due to characteristics of the wind speed pattern depending on the location or even due to the method and strategy adopted. Generally, if the forecast period is short, the wind speed forecast is more relaxed, and hence the errors are smaller. On the other hand, the forecast errors are larger in long-term forecasting [34].

### 5. RESULTS AND DISCUSSION

The training performance and regression are not reported here for all the cases. Rather performance validation, regression, error autocorrelation, and time-series responses are included for the first case only in Figure 8, Figure 7, Figure 9, and Figure 10; respectively. It is to be mentioned that the datasets used in each location do not correlate with each other because of the distinct geographical locations. Hence, the learning capability of the models developed for each case has no effect on the prediction results of other locations. The MSE for 77 epochs (Figure 7) shows that the errors stabilized after 8 epochs, and the testing values fall near the best possible values and match with the validation line. The scatter plots between the output and the target (measured) values showed a correlation of around 0.99 for training, validation, testing, and validation for output targets of  $\pm 0.019$ ,  $\pm 0.016$ ,  $\pm 0.059$ , and  $\pm 0.025$ , see Figure 8. Furthermore, correlation versus lag (Figure 9) demonstrated a normal distri-

bution. The time-series trends of target, training, validation and errors for each data points are shown in Figure 10 and are found in close agreement with each other.

**5.1 Case I:** Wind speed is the only input parameter in Case I. The model is developed using the dataset for 4 years from 2011 to 2014 and tested with the data for 2015 from 2017 to predict wind speeds for the year 2018. The error metrics obtained in this case are given in Table 1. The error estimates (Table 1) show minimum values for Khafji, followed by Jubail and Dhahran. Moreover, the errors recorded in Case I are higher than those for other cases as will be discussed in forthcoming sections. These higher values may be accounted for the long-term prediction of local weather conditions. To support this claim, it is worth mentioning that at Khafji site, the average wind speed is higher than that at the other two sites.

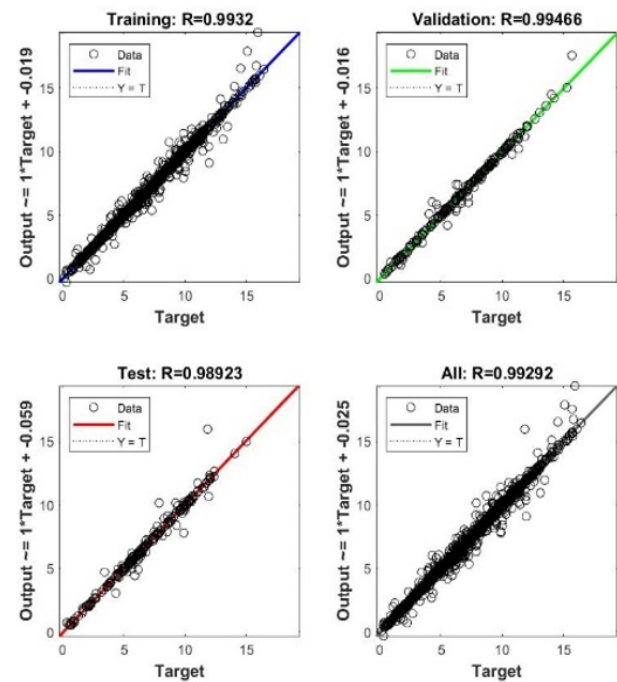


Figure 7. Training regression, Case 1.

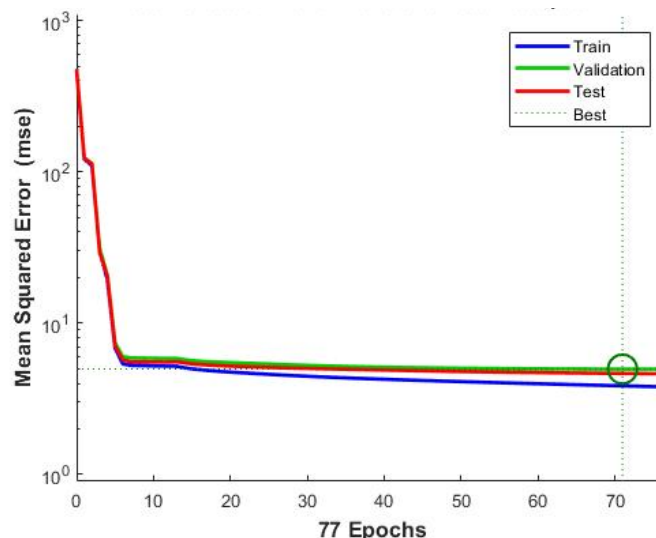


Figure 8. Performance validation, Case 1.

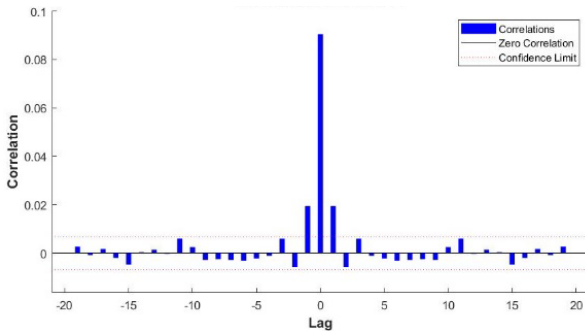


Figure 9. Error correlation, Case 1.

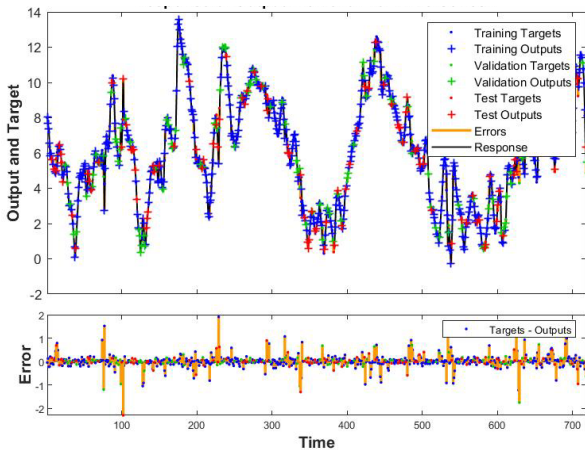


Figure 10. Time series response, Case 1.

Table 1. Error metrics in Case 1.

Metrics/Location	Dhahran	Jubail	Khafji
MAE	3.81	2.50	2.31
MSE	55.96	11.63	8.46
RMSE	7.48	3.41	2.91

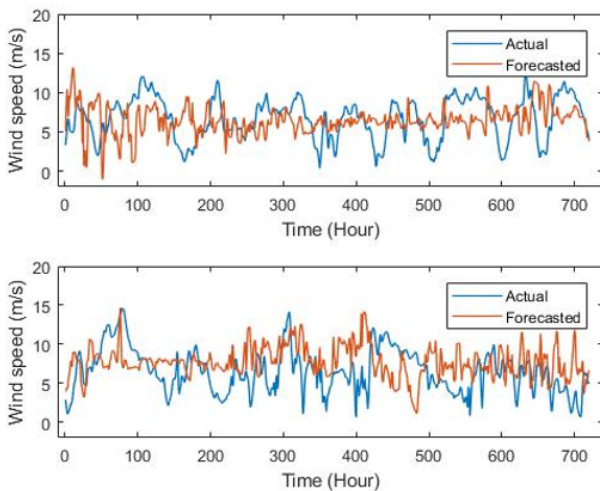


Figure 11. Forecasted and measured wind speeds for 2017, Jan & Feb. Dhahran, Case I.

The measured and the forecasted wind speed values show a near-to-close agreement and, more importantly, follow the increasing and decreasing trend in Dhahran during Jan & Feb, as shown in Figure 11. In Feb, the predicted wind speed values are better than those in Jan at Dhahran. At Jubail in Jan 2017, the predicted values

are in good agreement with measured values, as seen from the upper portion of Figure 12. Similar close or near matching trends between the measured and predicted wind speeds, except for some erratic values between 450 to 500 hours, are observed for Jubail in Feb 2017 (Figure 12). It is observed that the measured and the forecasted patterns in Figure 13 for Khafji during Jan and Feb 2017 are much closer than those at Dhahran and Jubail sites. In January at Khafji, the hourly mean values are in close agreement throughout 700 values with few erratic outliers. This trend is, however not obvious in Jubail.

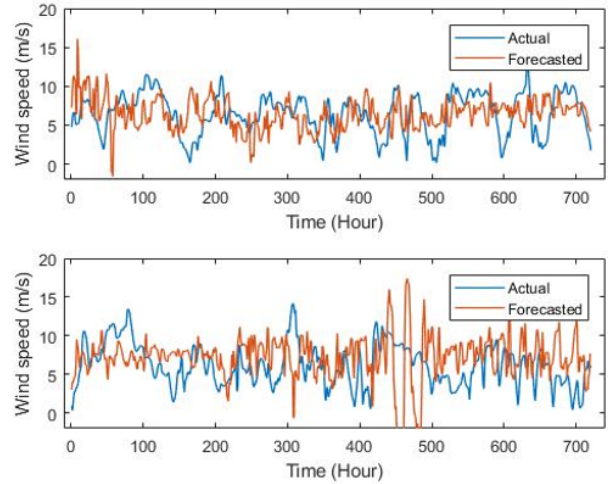


Figure 12. Forecasted and actual wind speeds of 2017, Jan & Feb, Jubail Case I.

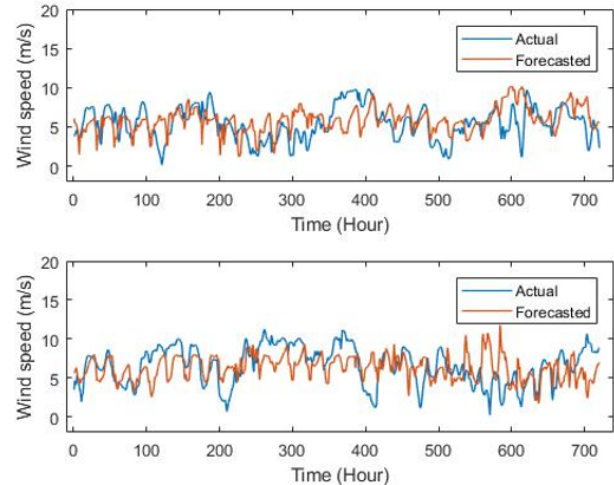


Figure 13. Forecasted and actual wind speeds of 2017, Jan & Feb, Khafji Case I.

**5.2 Case II:** In this case, temperatures at 2 and 10 m above ground level are added as training inputs in addition to the wind speed. The error metrics values summarized in Table 2 show lower values for Dhahran and little higher-ups for Jubail and Khafji, which may be accounted for variations in temperature values at these sites. The forecasted patterns in Dhahran showed a close agreement with the measured values in Jan (Figure 14-upper part) compared to that in Feb (Figure 14-lower part). In February, the model slightly overestimated the wind speed values except around 350 and 700 hours, where it underestimated the values (Figure 14-lower

portion). In July at Dhahran, initially from 0 to 100 hours, the model overestimated the wind speed and then underestimated it from 200 to 250 hours. Still, it is worth noting the increasing, and decreasing trends followed the measurements (Figure 15-upper part). In July, however, predicted values closely followed the measures trend up to around 180 hours, and then a few underestimates were observed about 200 hours (Figure 15-lower part). Between 380 and 460 hours, excellent agreement is seen between the two.

In January and February for Jubail data set, wind speed estimates in February (Figure 16-lower part) followed the increasing and decreasing trends of the measured values very closely. However, in January (Figure 16-upper part) the results were not encouraging but generally followed the trend with over and underestimations. Furthermore, at Jubail during June and July, matching decreasing and increasing trends of wind speeds between measured and estimated values are observed with some over- and underestimations (Figure 17).

**Table 2. Error metrics in Case II.**

Metrics/Location	Dhahran	Jubail	Khafji
MAE	3.00	2.93	2.99
MSE	14.58	13.60	14.26
RMSE	3.82	3.69	3.78

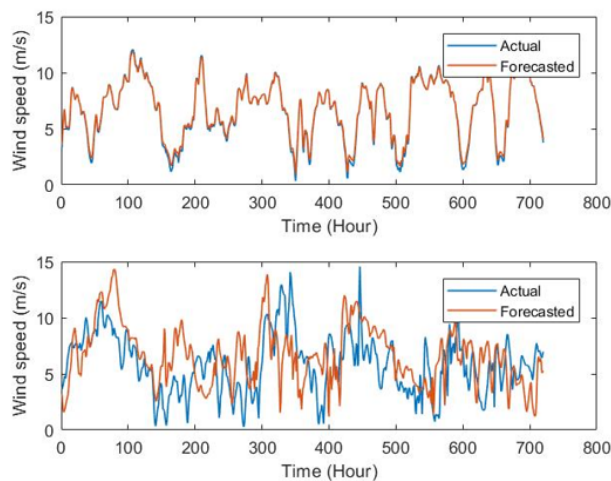


**Figure 14. Forecasted and actual wind speeds of 2017, Jan & Feb, Dhahran Case II.**

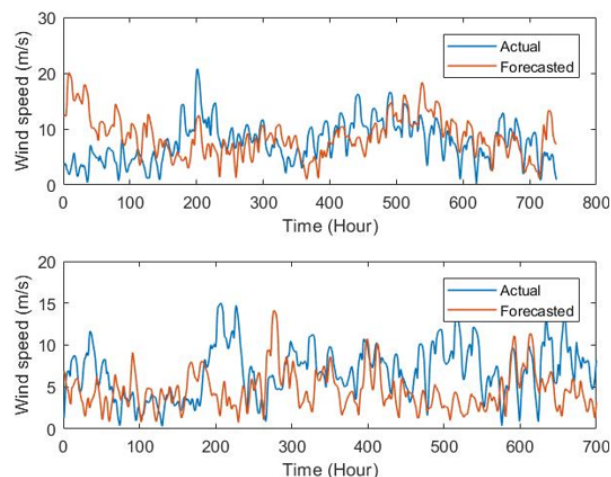


**Figure 15. Forecasted and actual wind speeds of 2017, Jun & July, Dhahran, Case II.**

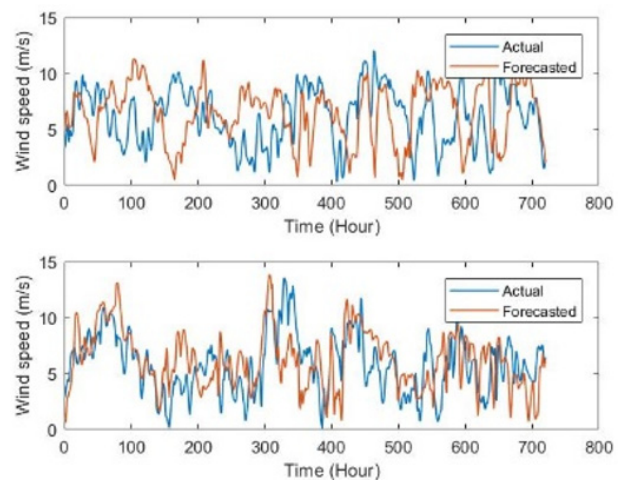


**Figure 16. Forecasted and actual wind speeds of 2017, Jan & Feb, Jubail, Case II.**

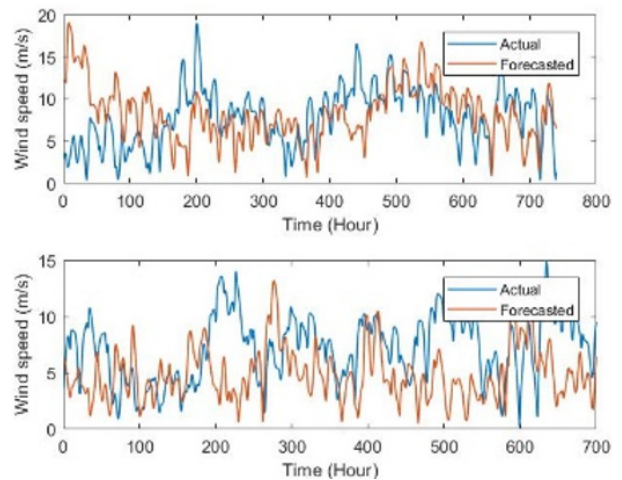


**Figure 17. Forecasted and actual wind speeds of 2017, Jun & July, Jubail, Case II.**

For Khafji data sets of June and July (Figure 18), an excellent comparison is observed between predicted and measured values during 200 to 400 hours and 480 to 600 hours (Figure 18-upper part). Some overestimations are observed between 0 to 150 hours and visible underestimations around 440 hours and between 600 and 700 hours. In July (Figure 18-lower part), the model underestimated the values for most of the time shown in this figure.

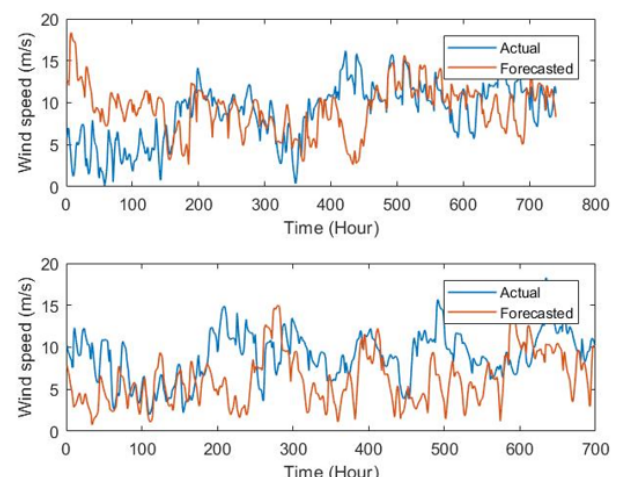


**Figure 18. Forecasted and actual wind speeds of 2017 Jun & Jul, Khafji, Case II.**

**5.3 Case III:** In this case, the input training parameters include wind speed, temperatures, and pressure values. The error metric, in this case, is summarized in Table 3. It shows better performance than the previous two cases. The average MAE, MSE, and RMSE for all sites are approximately the same and lower than those given in Table 1 and Table 2.

**Table 3. Error metrics in Case III.**

Metrics/Location	Dhahran	Jubail	Khafji
MAE	2.47	2.34	2.42
MSE	9.70	8.58	9.06
RMSE	3.12	2.93	3.01

During January and February data sets at Dhahran, the estimated values are seen in very close agreement with the measured ones in January (Figure 19-upper part). An excellent trend-following pattern is observed in February with acceptable under and overestimations (Figure 19-lower part). In June, an excellent trend-following and a close agreement are observed between the estimated and the measured values throughout the data length except between 0 and 100 hours. The model overestimated wind speeds (Figure 20-upper part). In July, the model underestimated wind speeds but followed the increasing and decreasing trend of measured wind speed values (Figure 20-lower part). The patterns in Jan/Feb and Jun/Jul are closely matched to the measured patterns. The closeness is much more pronounced in January and June than in February and July.

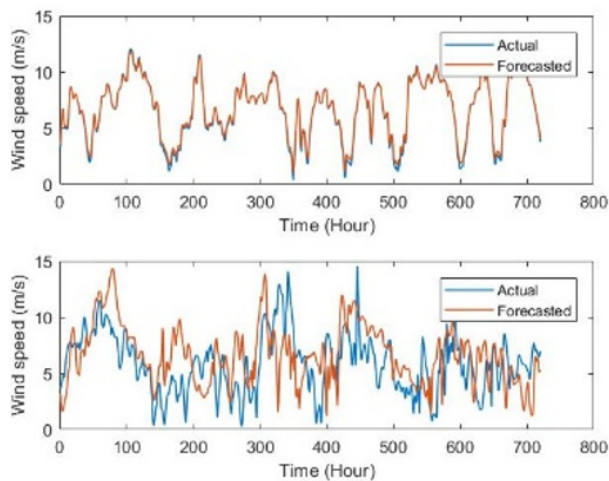


**Figure 19. Forecasted and actual wind speeds of 2017, Jan & Feb, Dhahran, Case III.**

Similarly, at Jubail site, Figure 21 and 22 show that the variability of characteristics of the wind speed patterns in January/February and June/July follow the increasing and decreasing trends closely with each other. However, the closeness between the predicted and measured wind speed values are better in February (Figure 21-lower part) and June (Figure 22-upper part) relative to January (Figure 22-upper part) and July (Figure 22-lower part). At Khafji in January (Figure 23-upper part), the model over- and underestimated the values but mostly followed the trend. In February (Figure 23-lower part), the predicted values remained near the measured ones and followed the increasing and decreasing trend satisfactorily. Similarly, more or less the same agree-

ment between the predicted and measured wind speed values is observed in June and July at Khafji (Figure 24). Relatively better agreement is observed in February (Figure 23-lower part) and June (Figure 24-upper part) compared to January and July at Khafji.

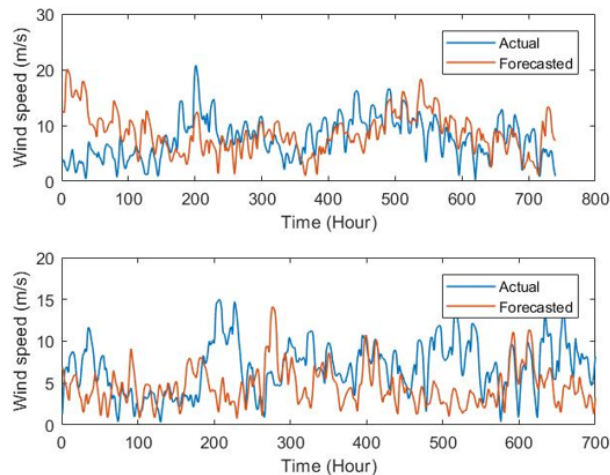


**Figure 17. Forecasted and actual wind speeds of 2017, June & July, Dhahran, Case III.**

In most examples, the forecasts agree with the measured values and follow the essential trends, whereas wind speed predictability strength is concerned.

## 6. CONCLUSIONS

The study found that NARNN is a viable tool for long-term wind speed prediction. It is observed that the accuracy of NARNN improved with increasing the number of training exogenous features. However, the method requires including the wind speed as part of the training input for improved accuracy. The accuracy of prediction by NARNN has limitations for long-term prognosis. The model captures the impact of seasons and the wind speed pattern repeatability. Still, more significant discrepancies are observed while comparing the predicted and measured values trends in this Case I.

The addition of exogenous parameters like ambient temperatures at 10 and 2 m above ground level and the wind speed values improved the error metrics (model NARXNN1). For example, in Case II, the MAE, MSE, and RMSE values decreased to 3.0, 14.58%, and 3.82 m/s compared to corresponding values of 3.81, 55.96%, and 7.48 m/s in Case I.

In Case III (model NARXNN2) included exogenous parameters temperatures at 10 and 2 m and pressure near ground level along with the wind speed as inputs and wind speed as output, further improving the model's predictability compared to NARNN and NARXNN1. It can be understood from the lower values (2.47, 9.70%, and 3.12 m/s) of the error metrics MAE, MSE, and RMSE compared to the corresponding higher values of 3.00, 14.58%, and 3.82 m/s for Dhahran.

So, it can be concluded that based on the present scope of work, the addition of exogenous parameters does help in improving the model's predictability.

Geographical location plays a role in the predictive accuracy of wind speed, as observed from the simulation results. For example, in Case I, the MAE

decreases from 3.81 to 2.50 and to 2.31, corresponding to geographical locations Dhahran, Jubail, and Khafji; respectively.

Finally, the study concludes that long-term wind speed prediction requires special preparation and selection of the training data due to the repeatability of certain exogenous parameters and the wind speed itself. In future studies, other algorithms like long-short term memory neural network, transformer, ensemble sequence models can also be implemented on the same strategy.

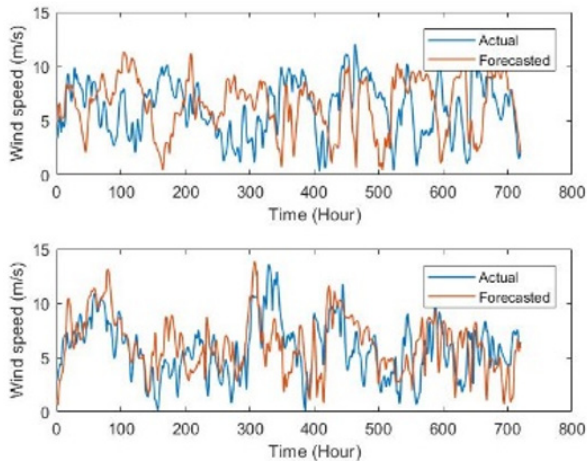


Figure 18. Forecasted and actual wind speeds of 2017, Jan. & Feb. Jubail, Case III.

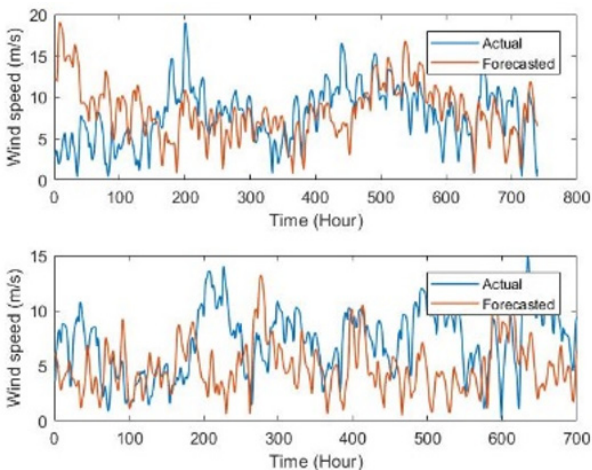


Figure 19. Forecasted and actual wind speeds of 2017, June & July, Jubail, Case III.

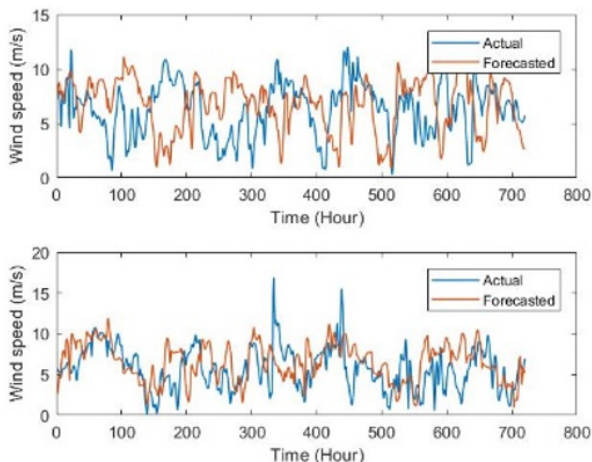


Figure 20. Forecasted and actual wind speeds of 2017, Jan. & Feb. Khafji, Case III.

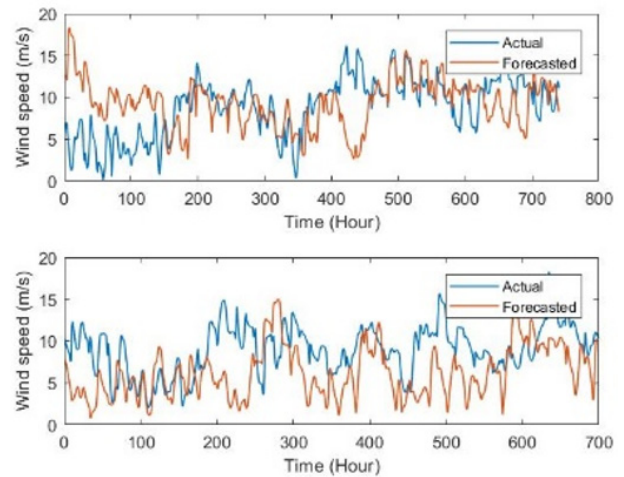


Figure 21. Forecasted and actual wind speeds of 2017, June & July, Khafji, Case III.

## ACKNOWLEDGEMENTS

Support of Deanship of Scientific Research, KFUPM, Saudi Arabia, for providing financial grant number DF191002 is acknowledged.

## REFERENCES

- [1] Sarkar R, Julai S, Hossain S, Chong WT, Rahman M. A comparative study of activation functions of NAR and NARX neural network for long-term wind speed forecasting in Malaysia. *Math Probl Eng* 2019;2019.
- [2] Rašuo BP, Bengin A. Optimization of wind farm layout. *FME Transactions* 2010; 38:107–14.
- [3] Rašuo B, Bengin A, Veg A. On Aerodynamic Optimization of Wind Farm Layout. *PAMM Proc Appl Math Mech* 2010; 10:539–40.
- [4] Rašuo B, Dinulović M, Veg A, Grbović A, Bengin A. Harmonization of new wind turbine rotor blades development process: A review. *Renew Sustain Energy Rev* 2014; 39:874–82.
- [5] Marugán AP, Pedro F, Márquez G, María J, Perez P, Ruiz-hernández D. A survey of artificial neural network in wind energy systems. *Appl Energy* 2018;228:1822–36.
- [6] Salman UT, Al-Ismael FS, Khalid M. Optimal sizing of battery energy storage for grid-connected and isolated wind-penetrated microgrid. *IEEE Access* 2020;8:91129–38.
- [7] Rehman S, Salman UT, Alhems LM. Wind Farm-Battery Energy Storage Assessment in Grid-Connected Microgrids. *Energy Eng* 2020;117:343–65.
- [8] Mohammed B, Abdullah OI, Al-Tmimi AI. Investigation and analysis of wind turbines optimal locations and performance in Iraq. *FME Trans* 2020;48:155–63.
- [9] Khazem EAZ, Abdullah OI, Sabri LA. Steady-state and vibration analysis of a WindPACT 1.5-MW turbine blade. *FME Trans* 2019; 47:195–201.
- [10] Liu Y, Racah E, Correa J, Khosrowshahi A, Lavers D, Kunkel K, et al. Application of deep convo-

lutional neural networks for detecting extreme weather in climate datasets. ArXiv Prepr ArXiv 160501156 2016.

- [11] Sturm M, Wagner AM. Using repeated patterns in snow distribution modeling: An Arctic example. *Water Resour Res* 2010;46.
- [12] Ranson M. Crime, weather, and climate change. *J Environ Econ Manage* 2014;67:274–302.
- [13] Pfister C. Monthly temperature and precipitation in central Europe 1525–1979: quantifying documentary evidence on weather and its effects. *Clim since AD 1992*;1500:118–42.
- [14] Watson SJ. ES2009-90053 2018:1–8.
- [15] Yan ZW, Wang J, Xia JJ, Feng JM. Review of recent studies of the climatic effects of urbanization in China. *Adv Clim Chang Res* 2016;7:154–68.
- [16] Jiang Y, Luo Y, Zhao Z, Tao S. Changes in wind speed over China during 1956-2004. *Theor Appl Climatol* 2010;99:421–30.
- [17] Li Q, Li W, Si P, Xiaorong G, Dong W, Jones P, et al. Assessment of surface air warming in northeast China, with emphasis on the impacts of urbanization. *Theor Appl Climatol* 2010;99:469–78.
- [18] Wasilewski J, Baczynski D. Short-term electric energy production forecasting at wind power plants in. *Renew Sustain Energy Rev* 2017;69:177–87.
- [19] Salman U, Rehman S, Alawode B, Alhems L. Short Term Prediction of Wind Speed Based on Long-Short Term Memory Networks. *FME Trans* 2021;49:643–52.
- [20] Tian Z, Wang G, Ren Y. Short-term wind speed forecasting based on autoregressive moving average with echo state network compensation. *Wind Eng* 2020;44:152–67.
- [21] Liu M, Cao Z, Zhang J, Wang L, Huang C, Luo X. Short-term wind speed forecasting based on the Jaya-SVM model. *Int J Electr Power Energy Syst* 2020;121:106056.
- [22] Rehman S, Khan SA, Alhems LM. The Effect of Acceleration Coefficients in Particle Swarm Optimization Algorithm with Application to Wind Farm Layout Design. *FME Transactions* 2020.
- [23] Rehman S, Natarajan N, Mohandes MA, Alam MM. Latitudinal wind power resource assessment along coastal areas of Tamil Nadu, India. *FME Transactions* 2020;48:566–75.
- [24] Svorcan J, Trivković Z, Ivanov T, Baltić M, Pečković O. Multi-objective constrained optimizations of VAWT composite blades based on FEM and PSO. *FME Transactions* 2019;47:887–93.
- [25] Barbounis TG. et al. Long-term wind speed and power forecasting using local recurrent neural network models. *IEEE Trans Energy Convers* 2006;21:273–84.
- [26] Blanchard T, Samanta B. Wind speed forecasting using neural networks. *Wind Eng* 2020;44:33–48.
- [27] Yang Z, Wang J. A hybrid forecasting approach applied in wind speed forecasting based on a data

processing strategy and an optimized artificial intelligence algorithm. *Energy* 2018;160:87–100.

- [28] Ait Maatallah O, Achuthan A, Janoyan K, Marzocca P. Recursive wind speed forecasting based on Hammerstein Auto-Regressive model. *Appl Energy* 2015;145:191–7.
- [29] Barbounis TG, Theocharis JB. Locally recurrent neural networks for long-term wind speed and power prediction. *Neurocomputing* 2006;69:466–96.
- [30] Azad HB, Mekhilef S, Ganapathy VG. Long-term wind speed forecasting and general pattern recognition using neural networks. *IEEE Trans Sustain Energy* 2014;5:546–53.
- [31] Saudi Tourism Authority. The seasons and climate in Saudi. *Travel Announc* n.d.
- [32] Umar T, Salman SSA, MA. Intelligent Flexible Priority List for Reconfiguration of Microgrid Demands Using Deep Neural Network. 2019 IEEE Innov Smart Grid Technol - Asia (ISGT Asia) 2019.
- [33] Elsheikh AH, Sharshir SW, Abd Elaziz M, Kabeel AE, Guilan W, Haiou Z. Modeling of solar energy systems using artificial neural network: A comprehensive review. *Sol Energy* 2019;180:622–39. doi:10.1016/j.solener.2019.01.037.
- [34] Guo Z, Dong Y, Wang J, Lu H. The Forecasting Procedure for Long-Term Wind Speed in the Zhangye Area 2010;2010.

#### NOMENCLATURE

ANN	Artificial neural network
ARIMA	Autoregressive integrated moving average
GHG	Greenhouse gases
HAR	Heterogeneous autoregressive
MAE	Mean absolute error
MAPE	Mean absolute percent error
MLP	Multilayer perceptron
NARNN	Nonlinear autoregressive neural networks
NARXNN	Nonlinear autoregressive exogenous
NN	Neural network
RMSE	Root mean square error

---

#### ПРЕДВИЂАЊЕ БРЗИНЕ ВЕТРА ЗАСНОВАНО НА ДУГОТРАЈНОЈ МЕМОРИЈИ ПРИМЕНОМ НЕЛИНЕАРНЕ АУТОРЕГРЕСИВНЕ НЕУРОНСКЕ МРЕЖЕ

**С. Рехман, У.Т. Салман, М. Мохандес,  
Ф.А. Сулејман, С. Адетона, Л.М. Алхемс,  
М.А. Басир**

Глобално гледано, енергија ветра је технолошки зрела и комерцијално прихваћена технологија. Међутим, испрекидана и променљива брзина ветра отежава његово директно повезивање са мрежом. Постаје мање атрактиван са становишта квалитета и континуираног напајања. Ипак, на брзину ветра утичу метеоролошки параметри као што су температура, притисак и релативна влажност и може се боље предвидети коришћењем свих ових параметара

или неких од теза као улазних података. Пошто се временски услови одређеног месеца понављају отприлике после десет година, а понекад и из године у годину у зависности од географског положаја. Ова студија истражује грешке повезане са предвиђањем брзине ветра у одређеном календарском месецу користећи историјске податке истог календарског месеца у претходним годинама. Аутори предлажу стратегију за дугорочно предвиђање брзине ветра засновану на два модела нелинеарне ауторегресивне неуронске мреже, (1) нелинеарне ауторегресивне неуронске мреже и (2) нелинеарне ауторегресивне неуронске мреже са егзогеним улазима. Модели су

развијени обучавањем мрежа са средњим вредностима брзине ветра по сату током седам година, од 2011. до 2017. године, за три локације у источној провинцији Саудијске Арабије. Ови модели се користе за предвиђање брзине ветра за 2018. годину, а резултати се упоређују са измереним подацима. Ефикасност оба модела се оцењује узимањем у обзир утицаја егзогених параметара (температура и атмосферски притисак). Студија је открила да тачност предвиђања брзине ветра у дугорочним прогнозама зависи не само од локације већ и од поновљивости узорака за обуку током година.